Epilepsia Open® The Open Access Journal of the International League Against Epilepsy

Open Access

FULL-LENGTH ORIGINAL RESEARCH

Unravelling the brain networks driving spike-wave discharges in genetic generalized epilepsy—common patterns and individual differences

***Silke Klamer, †‡§Thomas Ethofer, *Franziska Torner, *†§Ashish Kaul Sahib, *§¶Adham Elshahabi, *Justus Marquetand, *Pascal Martin, *§Holger Lerche, †Michael Erb, and *§Niels K. Focke**

Epilepsia Open, 3(4):485–494, 2018
doi: 10.1002/epi4.12252

Silke Klamer is resident in the Department for Neurology and Epileptology at the University of Tübingen.

Summary

Objective: Genetic generalized epilepsies (GGEs) are characterized by generalized spike-wave discharges (GSWDs) in electroencephalography (EEG) recordings without underlying structural brain lesions. The origin of the epileptic activity remains unclear, although several studies have reported involvement of thalamus and default mode network (DMN). The aim of the current study was to investigate the networks involved in the generation and temporal evolution of GSWDs to elucidate the origin and propagation of the underlying generalized epileptic activity.

Methods: We examined 12 patients with GGE and GSWDs using EEG–functional magnetic resonance imaging (fMRI) and identified involved brain areas on the basis of a classical general linear model (GLM) analysis. The activation time courses of these areas were further investigated to reveal their temporal sequence of activations and deactivations. Dynamic causal modeling (DCM) was used to determine the generator of GSWDs in GGE.

Results: We observed activity changes in the thalamus, DMN, dorsal attention network (DAN), salience network (SN), basal ganglia, dorsolateral prefrontal cortex, and motor cortex with supplementary motor area, however, with a certain heterogeneity between patients. Investigation of the temporal sequence of activity changes showed deactivations in the DMN and DAN and activations in the SN and thalamus preceding the onset of GSWDs on EEG by several seconds. DCM analysis indicated that the DMN gates GSWDs in GGE.

Significance: The observed interplay between DMN, DAN, SN, and thalamus may indicate a downregulation of consciousness. The DMN seems to play a leading role as a driving force behind these changes. Overall, however, there were also clear differences in activation patterns between patients, reflecting a certain heterogeneity in this cohort of GGE patients.

KEY WORDS: Genetic generalized epilepsy, Generalized spike-wave discharges, Default mode network, Thalamus, Dynamic causal modelling.

Accepted July 24, 2018.

*Department of Neurology and Epileptology, Hertie-Institute for Clinical Brain Research, University of Tübingen, Tübingen, Germany; †Department of Biomedical Magnetic Resonance, University of Tübingen, Tübingen, Germany; ‡Department of Psychiatry and Psychotherapy, University of Tübingen, Tübingen, Germany; §Werner Reichardt Centre for Integrative Neuroscience, Tübingen, Germany; and ¶MEG Center, University of Tübingen, Tübingen, Germany

Address correspondence to Silke Klamer, Department of Neurology and Epileptology, Hertie-Institute for Clinical Brain Research, University of Tübingen, Hoppe-Seyler-Strasse 3, 72076 Tuebingen, Germany. E-mail: silke.klamer@uni-tuebingen.de

Key Points

- Networks involved in the generation and temporal evolution of generalized spike-wave discharges (GSWDs) were investigated using EEG-fMRI
- Deactivations in default mode network and dorsal attention network and activations in salience network and thalamus precede onset of GSWDs
- Also clear differences in activation patterns between patients were observed, indicating considerable heterogeneity
- Effective connectivity analysis indicates that default mode network gates GSWDs in genetic generalized epilepsies.

Genetic generalized epilepsies (GGEs) are a group of genetically determined disorders characterized by generalized spike-wave discharges (GSWDs) in electroencephalography (EEG) recordings without underlying structural brain lesion. Neurophysiologic and neuroimaging studies during the last decades have identified the thalamus and cortical regions as playing a major role as a driving source behind seizure and GSWD generation.[1–7] Therefore, it has been postulated that a cortico-subcortical network is involved in the initiation and maintenance of GSWDs.[8] EEG–functional magnetic resonance imaging (fMRI) has been used to investigate the temporal sequence of blood oxygen level–dependent (BOLD) signal changes. Several groups described changes in cerebral activity preceding the GSWDs seen in EEG by several seconds.[5,7,9–12] However, there seems to be significant variability in the timing and localization of these changes between patients. Brain areas consistently involved are the thalamus and areas belonging to the so-called default mode network (DMN), consisting of the ventral and dorsal medial prefrontal cortex, posterior cingulate cortex, the adjacent precuneus, and the lateral parietal cortex.[13] Furthermore, marked differences between the standard hemodynamic response function (HRF) used in conventional fMRI analyses and the actual BOLD time course in different brain regions of patients with GGE have been described.[11]

To further elucidate the networks involved in the pathogenesis of GGE, the functional connectivity strength (FCS) in resting-state networks between patients with GGEs and healthy controls have been compared.[14,15] Differences were observed within the supplementary motor area (SMA), the premotor cortex, the pulvinar, the ventrolateral thalamic nucleus, the DMN, the dorsal attention network (DAN, i.e., bilateral intraparietal sulcus, frontal eye field, and middle temporal lobe), and the salience network (SN, i.e., anterior insula, cingulate cortex, and temporal-parietal junction area).[14,15] This closes the loop between network studies and source analysis studies by summarizing the areas involved in GSWDs and assigning them to well-characterized brain networks.

However, the actual driving force behind GSWDs still remains unclear. Vaudano et al.[16] used dynamic causal modelling (DCM) to investigate the effective connectivity between 3 preselected regions (precuneus, thalamus, and prefrontal cortex) in 7 patients with GGEs. They found evidence that it was the activity in the precuneus gating GSWDs in the investigated network.

We took this one step further and used a data-driven approach to identify the networks involved in the generation of GSWDs. In a first step, we identified brain areas and networks involved in GSWDs in 12 patients with GGE using a classical event-related EEG-fMRI analysis. As it has been shown that the standard HRF differs markedly from the actual BOLD time course in patients with GGEs,[11] we investigated the temporal sequence of activity changes by analyzing the actual BOLD time courses. Finally, we further quantified the propagation pattern of GSWDs among the identified networks using DCM.

Materials and Methods

Subjects

We recruited 12 patients (11 female, mean age 36.9 years, standard deviation [SD] 17.14, range 21–75) from the Department of Neurology and Epileptology of the University Hospital Tübingen, who were diagnosed with GGE according to the International League Against Epilepsy (ILAE) 2006 classification scheme[17] and who showed GSWD during the EEG-fMRI measurement. The sample size was limited by the last inclusion criterion as in many adult patients with GGE the epilepsy is well controlled by medication so that they no longer showed GSWDs in the EEG. Further details regarding patient characteristics can be found in Table 1.

The study was approved by the ethics committee of the University of Tübingen in accordance with the guidelines of the Declaration of Helsinki. All participants gave written informed consent.

Data acquisition—simultaneous high-density EEG-fMRI recording

Simultaneous high-density (hd-) EEG-fMRI was recorded using a 256-channel EEG system (Electrical Geodesics, Inc., Eugene, OR, U.S.A.) within a 3 T Scanner (Siemens MAGNETOM Trio (10 patients), which was upgraded to a Siemens Prisma during the course of our study (2 patients, see Table 1 for details) (Siemens AG, Erlangen, Germany). EEG electrode impedances were kept below 50 kOhms. Foam pads were used to minimize motion and help secure patient comfort. Hd-EEG data were transmitted via fiberoptic cable from the amplifier located

Table 1. Demographic data of patients

Patient	Age (years)/sex	Diagnosis	AEDs	No. of events (GSWDs)	No. of seizures per month
1	28/F	GGE	LEV	11	0
2	45/F	GGE	ESL, LEV	9	0
3	59/F	JAE	LTG, TPM	8	0.3
4[a]	29/M	GGE	VPA, LEV	1	0
5[a]	23/F	GGE	LTG	11	0.08
6	21/F	JME	LEV	2	0.08
7	75/F	GGE	TPM, LTG	16	0.04
8	37/F	GGE	LEV	14	0
9	22/F	GGE	LTG	10	1
10	26/F	GGE	LEV	10	0
11	51/F	JME	LTG	4	0
12	27/F	CAE	No AEDs	8	0

N = 12.

AEDs, antiepileptic drugs; CAE, childhood absence epilepsy; ESL, eslicarbazepine acetate; F, female; GGE, genetic generalized epilepsy; JAE, juvenile absence epilepsy; JME, juvenile myoclonic epilepsy; LEV, levetiracetam; LTG, lamotrigine; M, male; TPM, topiramate; VPA, valproate.

[a]Indicates patients scanned on the Prisma

next to the scanner to a computer outside the scanner room. We acquired a sagittal T1-weighted 3 dimensional magnetization prepared rapid acquisition gradient echo (3D-MPRAGE) sequence as a high-resolution anatomic reference (repetition time [TR] 2.3 s, echo time [TE] 3.03 msec, flip angle (FA) 8 degrees, voxel size $1 \times 1 \times 1$ mm); a B_0 field map was recorded for later correction of distortions in the functional images caused by magnetic field inhomogeneity. For the functional sequence, 30 min of resting-state EEG-fMRI were acquired consisting of 900 gradient-echo planar T2*-weighted images covering the whole brain (TR 2 s, TE 32 msec, FA 90 degrees, voxel size $3 \times 3 \times 4$ mm) with simultaneous hd-EEG (sampling rate 5 kHz). The first 5 images of each experimental run were discarded in order to reach equilibrium of magnetization.

Data analysis

Preprocessing

Hd-EEG-data were off-line corrected for MR- and cardioballistic artifacts using Net Station software (Electrical Geodesics, Inc., Eugene, OR, U.S.A.). Onset and duration of GSWDs were marked by an experienced EEG reader upon visual inspection, and the exact time points were used for further analysis. fMRI data were analyzed in MATLAB (http://www.mathworks.com) using Statistical Parametric Mapping (SPM 12, Wellcome Trust Centre for Imaging Neuroscience; http://www.fil.ion.ucl.ac.uk/spm). Images were converted into Neuroimaging Informatics Technology Initiative (NIFTI-1) format. The functional imaging time series of each subject underwent slice time correction, was realigned and unwarped based on the estimated field map data, co-registered to the anatomic reference image and normalized to Montreal Neurological Institute (MNI) space. The normalized data were smoothed with an isotropic Gaussian kernel (8 mm full-width at half maximum) and filtered with a high-pass filter with a cut-off time of 128 s. A quality check of the realignment parameters revealed that head movement remained <5 mm throughout the whole session and <2 mm between 2 scans for each subject.

fMRI statistical analysis and propagation analysis

A single-subject analysis was performed entering the onsets of all single GSWDs into a general linear model (GLM) and convolving them with the standard HRF in order to evaluate BOLD signal changes associated with GSWDs. Realignment parameters were added as regressors of no interest. In all subjects the duration of single GSWDs remained below 2 s (the repetition time interval); therefore onsets were entered as events with 0 s duration.

To examine propagation of GSWD-associated signal changes, that is, BOLD signal changes preceding and following the onset of GSWD visible in scalp EEG, the onset vector was shifted in steps of 2 s (corresponding to the TR) from 20 s before to 20 s after the actual onset of GSWD. This means, we created 21 separate first-level GLMs, one for each of the timepoints from −20 s to +20 s in relation to the onset of the GSWD, thus obtaining 21 T-maps for each patient with 2 s intervals between each other.

For each patient, results are reported at a height threshold of $p < 0.001$, uncorrected. Correction for multiple comparisons across the whole brain was assessed at cluster level ($p < 0.05$, corrected) using random field theory, and only clusters exceeding this corrected threshold were considered.

BOLD time course extraction and analysis

Given the ongoing discussion, if the canonical HRF is adequate in GSWD, we decided to investigate the BOLD time courses directly in a set of regions of interest (ROIs). A similar approach has already been taken by other authors.[11]

Based on the results of the single subject analyses and previous literature we defined the following brain areas as

ROIs for further analysis: thalamus, precuneus (PREC), and medial prefrontal cortex (mPFC) as parts of the DMN[13]; frontal eye field (FEF) and superior parietal cortex with intraparietal sulcus (IPS) as belonging to the DAN,[18] and finally the anterior insula (AI) and the anterior cingulate cortex (ACC) as parts of the SN[19] (Fig. 2). Masks for all these ROIs were created using an anatomic atlas.[20] To examine only BOLD signals from the gray matter, we created gray matter masks for each ROI. We used the individual gray matter probability masks generated during segmentation and averaged them across subjects. Only voxels with a tissue probability >0.5 for gray matter were included in the analysis. We then multiplied each binary mask of our ROIs with the mean gray matter mask of all 12 patients to obtain a gray matter mask for each ROI.

BOLD time courses, that is, the first principal eigenvariate of the voxel time series, were extracted for each patient within each ROI and mean-corrected using the "effects of interest" F-contrast. We used the first principal eigenvariate and not the average to get a summary of the responses within an ROI, because it does not assume homogenous responses within the ROI. For example, if half the ROI is activated and the other half deactivated, the average of the signal will be near zero, whereas the eigenvariate uses the temporal covariance of voxels in the ROI to show the activity.[21] The adjustment of the time series using the "effects of interest" F-contrast was done according to the instructions described in the SPM manual https://www.fil.ion.ucl.ac.uk/spm/doc/manual.pdf, (p. 317/318).

Time courses were extracted from 14 s before to 14 s after the onset of the GSWD. This shorter time window was chosen for reasons of clarity based on the results of the GLM single-subject analyses. Significant signal changes were observed in the interval between −20 s and +8 s in the GLM analysis. The hemodynamic response function, on which the GLM analysis is based, peaks at 6 s; therefore we adapted the interval for the direct analysis of the BOLD signal to −14 s (−20 + 6) until +14 s (+8 + 6). Overlapping segments, that is, segments containing GSWD less than 28 s apart, were discarded. As baseline, BOLD time courses of equal length, that is, 28 s duration, were extracted from time periods with a distance of at least 14 s to GSWD so as not to overlap with the above-described segments. We chose an equal number of baseline segments as GSWD segments for each subject. Three of our patients demonstrated only a few (i.e., 1, 2, and 4) GSWD (Table 1). In these cases, we increased the number of baseline segments to 8, which corresponds to the lowest number of segments in the remaining patients. The difference between the time courses of GSWDs and baseline was obtained by subtracting the respective segments (analogous to the contrast GSWD vs. rest in the GLM analysis). To demonstrate co-fluctuation of ROIs belonging to the same resting-state network (RSN, i.e., between PREC and mPFC, FEF and IPS, and AI and ACC) we calculated correlation coefficients for both GSWD and baseline segments. To test whether each 2 ROIs co-fluctuate significantly, we performed one-sample *t*-tests ($p < 0.05$) of Fisher-Z transformed correlation coefficients across subjects. Means and standard errors of the means (SEMs) of correlation coefficients were calculated from individual Fisher-*Z* scores and subsequent back-transformation to correlation coefficients.

DCM on single subject and group level

To answer the question of the driving force behind GSWDs in GGEs, we performed effective connectivity analyses using the DCM module in SPM 12 between the thalamus and the 3 RSNs. Because we were able to demonstrate that the 2 ROIs belonging to one of our investigated RSNs co-fluctuate, we chose only one ROI per RSN, that is, thalamus, PREC, FEF, and ACC, for effective connectivity analysis to avoid constructing overly complex models. We used the mean-corrected first principal eigenvariate of the voxel time series for each ROI and compared 4 models, each with one of the ROIs receiving external input and reciprocal forward and backward connections between all ROIs (Fig. 3A). After estimation of the parameters of each model within each modality and for each patient, they were compared on single-subject and on group level using Bayesian model comparison, in which selection of the most appropriate model is made using the difference in their log-evidence scores with a difference of more than three being regarded as statistically significant.

Results

GLM analysis on single-subject level

GLM analysis on single-subject level revealed significant results for each patient (see Fig. 1 for the results of 3 exemplary subjects, Table S1 and Fig. S1 for all subjects). We observed marked interindividual differences regarding the time course of activity changes as well as the relation of activations and deactivations in affected regions and networks. Activity changes started 16 to 0 s before the actual onset of GSWDs in scalp EEG and lasted up to 8 s after onset at the given threshold. However, the affected brain areas and networks were similar throughout all patients. In detail, there was clear involvement of the thalamus, DMN, DAN, SN, basal ganglia, dorsolateral prefrontal cortex, and motor cortex with SMA. Of interest, likely due to the intersubject heterogeneity regarding the time course of activity changes and relation of activation and deactivations in the affected brain areas, second-level group analysis did not yield any statistically significant results.

Based on our first-level results and the previous literature, we chose the following 7 ROIs for all further analyses: thalamus, PREC and mPFC as part of the DMN, FEF, and IPS/superior parietal cortex as representing the DAN and the AI and ACC for the SN.

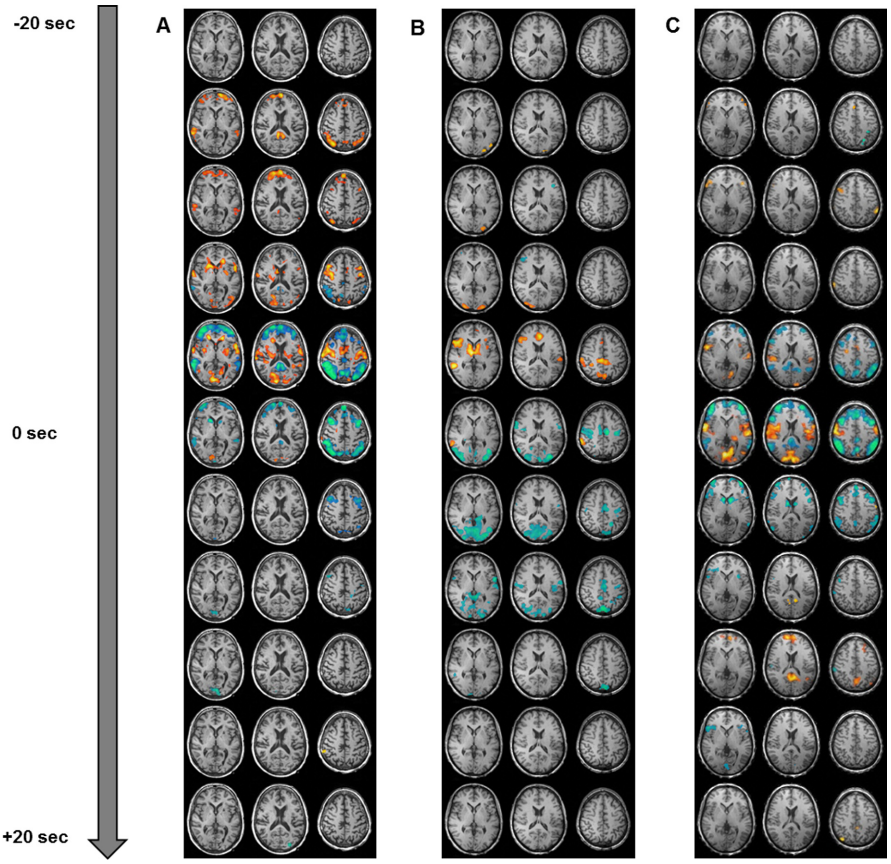

Figure 1.
Activation pattern of BOLD signal changes preceding and following GSWDs in 3 exemplary patients. Activations are depicted in yellow and deactivations in blue ($p < 0.05$, corrected at cluster level). (**A**) Patient 7, (**B**) Patient 11, and (**C**) Patient 12.

BOLD time-course analysis

The results of the mean BOLD time-course analysis of all patients for each ROI are depicted in Figure 2. They showed a BOLD signal increase in the thalamus beginning 2 s before the onset of GSWD reaching its plateau at 2 s after GSWD onset. An undershoot was observed beginning 10 s after GSWD onset. This corresponds relatively closely to the shape of the classical canonical HRF. In both DMN ROIs, that is, PREC and mPFC, the shape of the BOLD response was quite different: long lasting decreases were observed beginning at the onset of GSWD. In the mPFC, they were preceded by a slight activity increase starting 4 s before GSWD onset. The BOLD time course in the DAN ROIs paralleled the one in the DMN with long-lasting decreases beginning 2 to 0 s before GSWD onset. The time course in the SN on the other hand showed an increase beginning 2 s before and an undershoot at 10 s after GSWD, thus, very similar to the thalamic BOLD signal. Taken together, we observed increases in the thalamus and the SN and decreases in the BOLD signal in the DMN and the DAN beginning about 2 s before the actual onset of GSWD (see also Fig. S2).

We calculated the correlation coefficient between each 2 ROIs belonging to the same RSN, that is, PREC and mPFC (DMN), FEF and IPS (DAN), and AI and ACC (SN) (Table 2). These results indicate that the ROIs within one RSN co-fluctuate, enabling us to use only one ROI per RSN for the subsequent DCM analysis.

Effective connectivity/DCM analysis

Bayesian model comparison identified model 2, that is, neuronal activity originating in the PREC driving the other ROIs, to be significantly more likely than the other 3 models in the group analysis (Table S2, Fig. 3B). This is supported by the results of the single-subject analyses, which showed that model 2 is more likely than the other models in 6 patients. Model 3, that is, activity in the FEF driving the other ROIs, was identified as the best model in 3 patients. However, in all these patients, model 2 was the second best in explaining the data. Model 1, that is, thalamus as the driving force, was significantly better in 2 patients, whereas model 4 was the best in only 1 case. Figure S3 shows the relative log-evidence for the 4 models in each patient. Table S2 lists the *F* values, that is, the negative log-evidence as absolute value. Therefore,

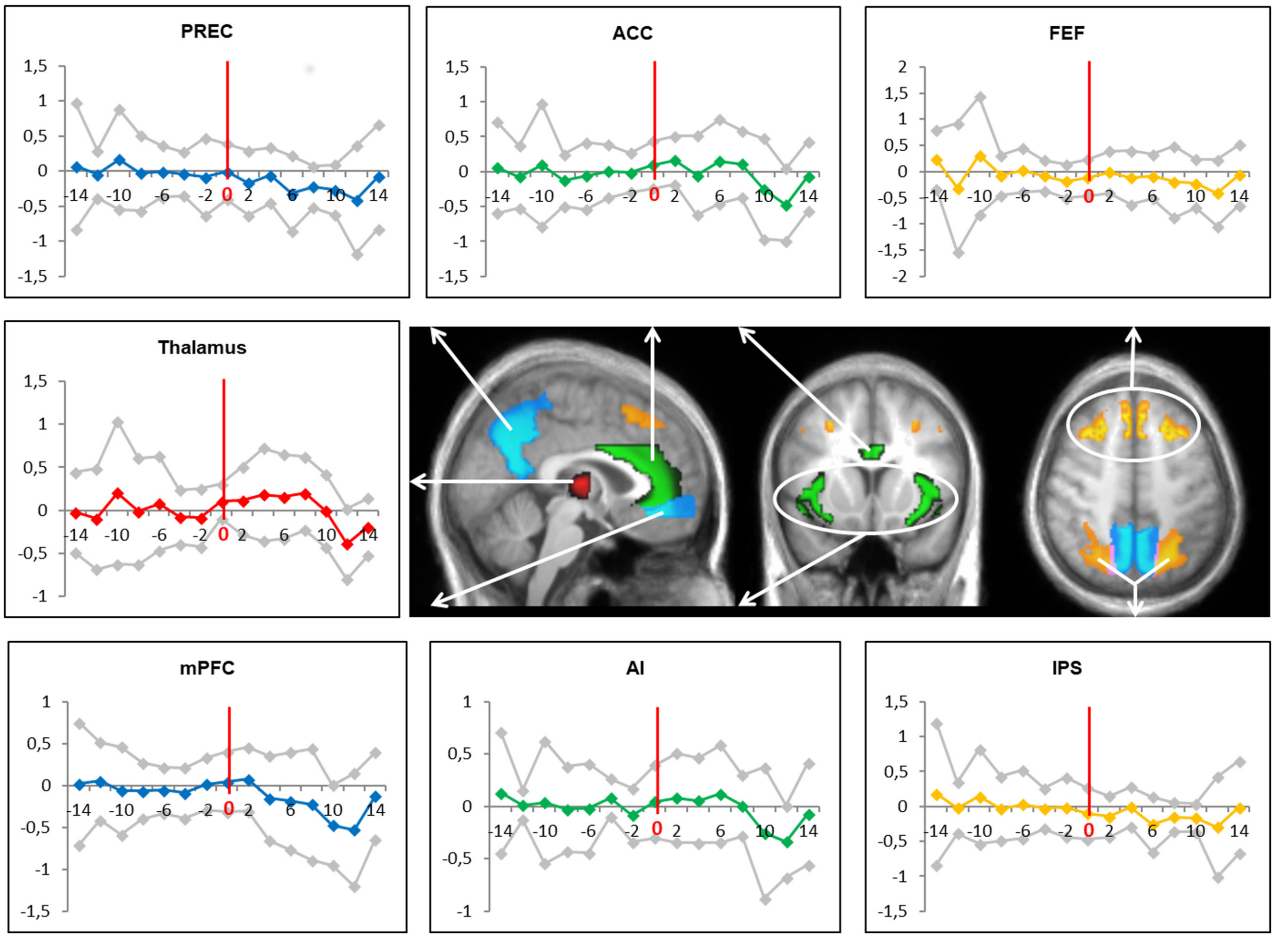

Figure 2.
Mean BOLD time courses during GSWDs. Mean BOLD time courses during GSWDs in the 7 ROIs are shown from −14 s to +14 s relative to GSWD onset. The colored lines represent mean BOLD time courses, and the gray lines represent standard deviations. PREC, precuneus; ACC, anterior cingulate cortex; FEF, frontal eye field; mPFC, medial prefrontal cortex; AI, anterior insula; IPS, superior parietal cortex with intraparietal sulcus.

despite some heterogeneity, these results suggest that key regions of the DMN, that is PREC and mPFC (see below), are the most likely source of GSWD generation in GGE patients.

Although the within-RSN correlation analysis showed good agreement of the different ROIs, we wanted to exclude that the choice of ROI for each RSN has influenced the results of the DCM analysis. Therefore, we recalculated the analysis with interchanged ROIs (i.e., mPFC instead of PREC, IPS instead of FEF and AI instead of ACC), which produced very similar results at single-subject level and equivalent results at group level (data not shown).

Discussion

Networks involved in GSWDs

As expected, GLM analysis revealed BOLD signal increases in the thalamus, which we observed in 6 patients at the given threshold. Lowering the threshold revealed thalamic activations in all patients (data not shown). There is agreement in the existing literature that the thalamus plays a pivotal role in the pathophysiology of GSWDs. Several studies have demonstrated thalamic activations during absence seizures in animals[8] and humans.[4–7,10–12,22–26] However, its exact role in triggering and/or maintaining GSWDs remains a matter of debate.[8,27] In a study with epileptic rats it has been demonstrated that seizures originate in the cerebral cortex, which then drives the thalamus,[27] suggesting that the thalamus represents rather a final pathway for GSWDs.

The DMN consists of medial prefrontal cortex, posterior cingulate cortex, and adjacent precuneus plus lateral parietal cortex. It is most commonly shown to be active when the brain is at wakeful rest and supports the state of consciousness. Activity in this network decreases in various goal-oriented tasks, which is why it is also called "task-negative network" (for review see[13]). It has been shown, that activity

Table 2. Correlation coefficients *r* between ROIs within RSN (in brackets) during GSWDs and baseline

	GSWD			Baseline		
Subject	ACC + AI (SN)	FEF + IPS (DAN)	mPFC + PREC (DMN)	ACC + AI (SN)	FEF + IPS (DAN)	mPFC + PREC (DMN)
Subject 1	0.45	0.32	0.85	0.69	0.77	0.36
Subject 2	0.43	0.76	0.89	0.72	0.70	0.73
Subject 3	0.87	0.56	0.55	0.80	0.75	0.61
Subject 4	0.47	0.31	0.04	0.23	0.58	0.82
Subject 5	0.69	0.21	0.66	0.53	0.17	0.70
Subject 6	0.86	0.70	0.66	0.70	0.61	0.49
Subject 7	0.78	0.63	0.63	0.86	0.67	0.33
Subject 8	0.83	0.43	0.62	0.27	−0.35	0.58
Subject 9	0.70	0.84	0.84	0.80	0.73	0.53
Subject 10	0.28	0.64	0.89	0.44	−0.37	0.70
Subject 11	0.75	−0.06	0.55	0.70	0.20	0.68
Subject 12	0.52	−0.23	0.73	0.76	0.52	0.36
Mean (SEM)	0.82 (±0.10)[b]	0.52 (±0.12)[b]	0.88 (±0.11)[b]	0.80 (±0.10)[b]	0.51 (±0.14)[a]	0.69 (±0.07)[b]

ACC, anterior cingulate cortex; AI, anterior insula; DAN, dorsal attention network; DMN, default mode network; FEF, frontal eye field; GSWDs, generalized spike-wave discharges; IPS, superior parietal cortex with intraparietal sulcus; mPFC, medial prefrontal cortex; PREC, precuneus; ROI, region of interest; RSN, resting state network; SN, salience network.

[a] $p < 0.01$

[b] $p < 0.001$

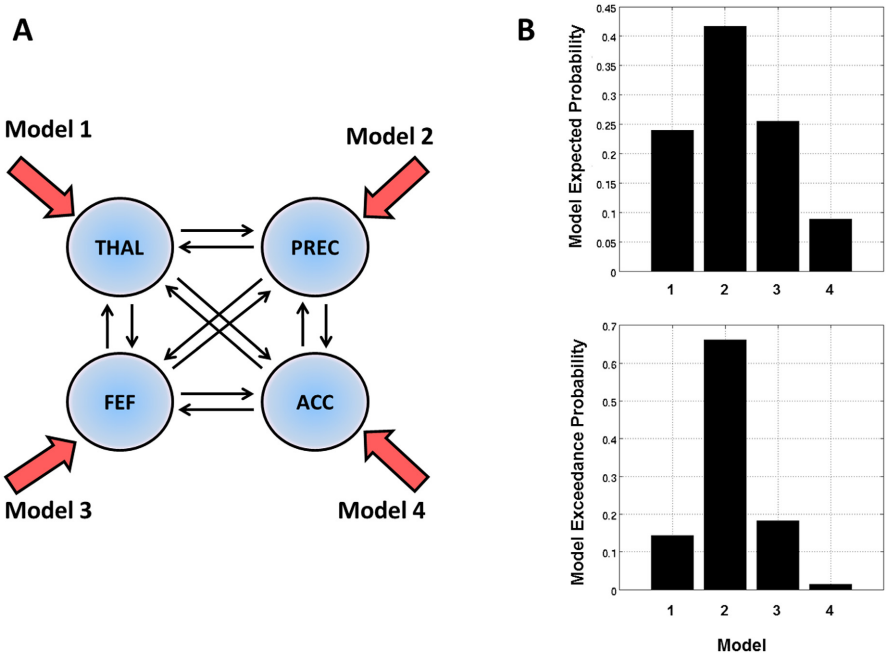

Figure 3.

Effective connectivity (DCM) models and group analysis. (**A**) All 4 ROIs are forward and backward connected. Red arrows show the node acting as autonomous input over the other ROIs in the 4 different models (Model 1 to 4). THAL, thalamus; PREC, precuneus; FEF, frontal eye field; ACC, anterior cingulate cortex. (**B**) Model comparison identified model 2 as being more likely than the other 3 models, that is, activity in the precuneus gates changes in the other ROIs.

in the DMN also decreases during absence seizures and GSWD.[2–7,10–12,16,24,25] This was discussed as hemodynamic correlate of impaired consciousness during absence seizures.[2–6,25] Network studies also revealed decreased functional network connectivity within the DMN during GSWDs,[28] as well as between DMN, SN, and DAN in patients with GGEs.[15] We observed activity changes in DMN regions in 83% of our patients. 40% of them demonstrated activations preceding the onset of GSWDs visible in EEG by several seconds followed by deactivations in the DMN around the time point of the onset of GSWDs. Thirty percent demonstrated only deactivations, and the remaining

30% only activations. This underscores the prominent role of the DMN in GSWDs, but also demonstrates the heterogeneity of activation patterns in a typical adult GGE patient cohort.

The role of the DAN in GGE is less well established. It consists of frontal eye field and intraparietal sulcus with adjacent superior parietal cortex and is involved in top-down processing by preparing and applying goal-directed selection for stimuli and responses.[18] We were able to identify involvement of the DAN in GSWDs in 50% of our patients: Most of them showed activations, one showed deactivations, and one patient demonstrated deactivations followed by activations. Altered functional connectivity within the DAN and between DAN and other RSNs has been described previously, underscoring the role of this network in the pathophysiology of GSWDs.[15,28,29]

The SN encompasses anterior insula and dorsal anterior cingulate cortex and activates in response to varied forms of salience, including emotion, homeostatic regulation, and reward.[19] Again, literature describing the role of the SN in GGE patients is scarce. We observed activity increases in the SN in 58% of patients. Network studies in GGE patients corroborate this finding in demonstrating altered connectivity within the SN and between this and other RSNs, such as DMN and DAN.[15,28,30,31] This might indicate altered processing of salient information in GGE patients and might be associated with attentional dysfunction during absence seizures.

Temporal sequence of activations and deactivations

Several studies in healthy subjects have provided evidence that the hemodynamic response may vary from one brain region to another and is not necessarily congruent with the canonical HRF used in a conventional GLM analysis.[32–35] Differences in time and shape between the canonical HRF and the actual BOLD time course have also been repeatedly reported in epilepsy patients.[11,36,37] Furthermore, several studies in GGE patients have reported fMRI signal changes preceding the onset of GSWD visible in scalp EEG by several seconds.[5,7,10–12] It has been hypothesized that the reason for this might be that the standard HRF does not correctly reflect the neurovascular coupling at all places and times and/or electrical events in the brain do not begin and end uniformly with scalp EEG signals.[11]

Thus, we analyzed the BOLD time course directly to unravel the temporal sequence and interplay of activations and deactivations in a set of ROIs identified using the standard GLM analysis. The group analysis revealed increases in the thalamus and the SN ROIs and decreases in the BOLD signal in the DMN and the DAN ROIs beginning about 2 s before the actual onset of GSWD. It is important to note that we did not apply any temporal shifting/convolution of BOLD time courses. Although the exact shape and temporal sequence is debatable, a certain delay of the BOLD/vascular signal and the true neuronal activity in the order of a few seconds is widely established. This indicates that neuronal (network) alterations robustly precede GSWD appearance by several seconds. Furthermore, although the thalamic activity changes resembled closely the shape of the canonical HRF, BOLD time courses in the other ROIs differed considerably. This observation is in line with the findings of Bai and colleagues,[11] who also observed a time course similar to the HRF model only in the thalamus, but no other investigated ROI. However, as in the GLM analysis, BOLD time-course analysis on a single-subject level revealed a considerable inter-individual heterogeneity that is reflected in relatively large standard deviations. The discrepancy in timing compared to the standard GLM analysis must therefore be attributed to the interindividual variability in fMRI activity changes and to the difference in the actual BOLD signal time course and the shape of the canonical HRF. Our results underscore the observation that a simple GLM analysis does not capture the whole spectrum of cerebral activity changes leading to GSWD. Although it seems appropriate for the identification of involved ROIs, it does not reveal the exact time course of GSWD-associated activity changes. One reason might be that the canonical HRF does not reflect the actual BOLD signal time course in all affected brain areas. Another reason could be that the activity preceding the GSWD does not constitute a brief event but rather a prolonged change in network activity leading up to—or "igniting"—the actual GSWD, which cannot be captured with a simple event-related analysis.

An interesting observation resulting from this analysis is the interplay between different RSNs. Although DMN and DAN seem to deactivate during GSWDs, thalamus and SN are activated. Intrinsic connections between thalamus and ROIs belonging to the SN have been demonstrated previously and were associated with sympathetic efference and interoceptive feedback.[19] It appears, therefore, that during GSWDs, conscious rest and top-down processing might be downregulated in favor of interoceptive-autonomic processing, which is mediated by the interplay between thalamus, FEF, and ACC.

Effective connectivity analysis reveals driving force behind GSWDs

DCM is a method to assess the effective connectivity between brain regions, that is, the causal influence that one neuronal system exerts over others.[38] It can be used to test which brain region drives which making it a very appealing tool in epilepsy diagnostics, where the main question is that of the actual focus or origin of epileptic activity. DCM has already been successfully used to investigate effective connectivity in epileptic networks on a single-subject patient-specific level,[39–42] as well as in a small group of patients with GGE.[16] The latter study investigated the effective connectivity between precuneus, thalamus, and prefrontal cortex to identify a causal hierarchy during GSWDs. Their results indicated, despite some interindividual differences,

that activity in the precuneus gates epileptic activity within a thalamocortical loop.

Our results extend these findings and indicate that GSWD is gated by neural activity of 2 key regions of the DMN, that is, precuneus and medial prefrontal cortex, even if a more complex model is employed including 3 RSNs (i.e., DMN, DAN, and SN) and the thalamus. However, on a single-subject level, we observed some differences in the causal hierarchy of networks driving the epileptic activity. This might be due to heterogeneity in this syndrome despite the seemingly homogeneous clinical phenotype. Future studies should investigate whether this heterogeneity is time-invariant and can be reliably found if the same patients are examined at different time points.

Clinical considerations

Our time course analysis revealed that changes in certain RSNs can occur up to 16 s before the actual onset of GSWDs, which offers a small time window in which detection and potentially therapeutic intervention, for example, by closed-loop electrostimulation, would be possible. However, bearing in mind the interindividual variability, this could only be achieved on a patient-specific level in the context of a personalized medicine concept.

Strengths and limitations

We obtained very robust results in the first-level analysis with significant activations and deactivations corrected at cluster level in every single patient. This indicated that the within-patient temporal sequence is similar between GSWDs. However, the GLM results were rather heterogeneous across patients, which might be due to the fact that our patient cohort included patients with different GGE syndromes and potentially different pathophysiologic mechanisms. Furthermore, our patient group differs also with regard to several other factors, as there are type of medication, age, duration of epilepsy, and number of GSWDs recorded. To distinguish the contribution of all these factors to the networks involved in GSWD generation, a larger cohort would be necessary. But also the investigation of a cohort with distinct underlying genetic mutation would be relevant. Therefore, the small sample size of 12 subjects has to be regarded as a limitation.

Conclusion

We were able to demonstrate marked interindividual differences in the time course of fMRI activations and deactivation leading toward GSWD in GGE. We found significant fMRI changes preceding the GSWD appearance in EEG by up to 16 s indicating that the epileptic activity does not appear "out of the blue" but has relevant buildup time in GGE. This could enable a window of opportunity for therapeutic intervention. Furthermore, we studied the brain networks involved in GSWD generation, that is, DMN, DAN, and SN, as well as the thalamus. During GSWD, DMN and DAN are deactivated, whereas SN and thalamus are activated, which may indicate a downregulation of consciousness. Effective connectivity analyses revealed key regions of the DMN, that is, precuneus and medial prefrontal cortex, as playing a leading role as driving force behind these changes offering a potential target for therapeutic interventions.

Acknowledgments

Silke Klamer was supported by the *fortüne*-Programm (2055-0-1) of the University of Tübingen. The study was further supported by the AKF-Programm (289-0-0) of the University of Tübingen, the Center for Integrative Neurosciences, and the Deutsche Forschungsgemeinschaft.

Disclosure

None of the authors have potential conflicts of interest to be disclosed. We confirm that we have read the Journal's position on issues involved in ethical publication and affirm that this report is consistent with those guidelines.

References

1. Avoli M. A brief history on the oscillating roles of thalamus and cortex in absence seizures. *Epilepsia* 2012;53:779–789.
2. Gotman J, Grova C, Bagshaw A, et al. Generalized epileptic discharges show thalamocortical activation and suspension of the default state of the brain. *Proc Natl Acad Sci USA* 2005;102:15236–15240.
3. Hamandi K, Salek-Haddadi A, Laufs H, et al. EEG-fMRI of idiopathic and secondarily generalized epilepsies. *NeuroImage* 2006;31:1700–1710.
4. Laufs H, Lengler U, Hamandi K, et al. Linking generalized spike-and-wave discharges and resting state brain activity by using EEG/fMRI in a patient with absence seizures. *Epilepsia* 2006;47:444–448.
5. Moeller F, Siebner HR, Wolff S, et al. Changes in activity of striato-thalamo-cortical network precede generalized spike wave discharges. *NeuroImage* 2008;39:1839–1849.
6. Moeller F, Siebner HR, Wolff S, et al. Simultaneous EEG-fMRI in drug-naive children with newly diagnosed absence epilepsy. *Epilepsia* 2008;49:1510–1519.
7. Carney PW, Masterton RA, Harvey AS, et al. The core network in absence epilepsy. Differences in cortical and thalamic BOLD response. *Neurology* 2010;75:904–911.
8. Blumenfeld H. Cellular and network mechanisms of spike-wave seizures. *Epilepsia* 2005;46(Suppl 9):21–33.
9. Hawco CS, Bagshaw AP, Lu Y, et al. BOLD changes occur prior to epileptic spikes seen on scalp EEG. *NeuroImage* 2007;35:1450–1458.
10. Moeller F, LeVan P, Muhle H, et al. Absence seizures: individual patterns revealed by EEG-fMRI. *Epilepsia* 2010;51:2000–2010.
11. Bai X, Vestal M, Berman R, et al. Dynamic time course of typical childhood absence seizures: EEG, behavior, and functional magnetic resonance imaging. *J Neurosci* 2010;30:5884–5893.
12. Benuzzi F, Mirandola L, Pugnaghi M, et al. Increased cortical BOLD signal anticipates generalized spike and wave discharges in adolescents and adults with idiopathic generalized epilepsies. *Epilepsia* 2012;53:622–630.
13. Raichle ME. The brain's default mode network. *Annu Rev Neurosci* 2015;38:433–447.
14. Ji GJ, Zhang Z, Xu Q, et al. Identifying corticothalamic network epicenters in patients with idiopathic generalized epilepsy. *AJNR Am J Neuroradiol* 2015;36:1494–1500.
15. Li Q, Cao W, Liao X, et al. Altered resting state functional network connectivity in children absence epilepsy. *J Neurol Sci* 2015;354:79–85.

16. Vaudano AE, Laufs H, Kiebel SJ, et al. Causal hierarchy within the thalamo-cortical network in spike and wave discharges. *PLoS ONE* 2009;4:e6475.
17. Engel J Jr. Report of the ILAE classification core group. *Epilepsia* 2006;47:1558–1568.
18. Corbetta M, Shulman GL. Control of goal-directed and stimulus-driven attention in the brain. *Nat Rev Neurosci* 2002;3:201–215.
19. Seeley WW, Menon V, Schatzberg AF, et al. Dissociable intrinsic connectivity networks for salience processing and executive control. *J Neurosci* 2007;27:2349–2356.
20. Tzourio-Mazoyer N, Landeau B, Papathanassiou D, et al. Automated anatomical labeling of activations in SPM using a macroscopic anatomical parcellation of the MNI MRI single-subject brain. *NeuroImage* 2002;15:273–289.
21. Friston KJ, Rotshtein P, Geng JJ, et al. A critique of functional localisers. *NeuroImage* 2006;30:1077–1087.
22. Salek-Haddadi A, Lemieux L, Merschhemke M, et al. Functional magnetic resonance imaging of human absence seizures. *Ann Neurol* 2003;53:663–667.
23. Labate A, Briellmann RS, Abbott DF, et al. Typical childhood absence seizures are associated with thalamic activation. *Epileptic Disord* 2005;7:373–377.
24. Benuzzi F, Ballotta D, Mirandola L, et al. An EEG-fMRI Study on the Termination of Generalized Spike-And-Wave Discharges in Absence Epilepsy. *PLoS ONE* 2015;10:e0130943.
25. Pugnaghi M, Carmichael DW, Vaudano AE, et al. Generalized spike and waves: effect of discharge duration on brain networks as revealed by BOLD fMRI. *Brain Topogr* 2014;27:123–137.
26. Guo JN, Kim R, Chen Y, et al. Impaired consciousness in patients with absence seizures investigated by functional MRI, EEG, and behavioural measures: a cross-sectional study. *Lancet Neurol* 2016;15:1336–1345.
27. Meeren H, van Luijtelaar G, Lopes da Silva F, et al. Evolving concepts on the pathophysiology of absence seizures: the cortical focus theory. *Arch Neurol* 2005;62:371–376.
28. Zhang Z, Liao W, Wang Z, et al. Epileptic discharges specifically affect intrinsic connectivity networks during absence seizures. *J Neurol Sci* 2014;336:138–145.
29. Wang Z, Lu G, Zhang Z, et al. Altered resting state networks in epileptic patients with generalized tonic-clonic seizures. *Brain Res* 2011;1374:134–141.
30. Dong L, Luo C, Zhu Y, et al. Complex discharge-affecting networks in juvenile myoclonic epilepsy: A simultaneous EEG-fMRI study. *Hum Brain Mapp* 2016;37:3515–3529.
31. Luo C, Yang T, Tu S, et al. Altered intrinsic functional connectivity of the salience network in childhood absence epilepsy. *J Neurol Sci* 2014;339:189–195.
32. Miezin FM, Maccotta L, Ollinger JM, et al. Characterizing the hemodynamic response: effects of presentation rate, sampling procedure, and the possibility of ordering brain activity based on relative timing. *NeuroImage* 2000;11:735–759.
33. Neumann J, Lohmann G, Zysset S, et al. Within-subject variability of BOLD response dynamics. *NeuroImage* 2003;19:784–796.
34. Handwerker DA, Ollinger JM, D'Esposito M. Variation of BOLD hemodynamic responses across subjects and brain regions and their effects on statistical analyses. *NeuroImage* 2004;21:1639–1651.
35. Meltzer JA, Negishi M, Constable RT. Biphasic hemodynamic responses influence deactivation and may mask activation in block-design fMRI paradigms. *Hum Brain Mapp* 2008;29:385–399.
36. Grouiller F, Vercueil L, Krainik A, et al. Characterization of the hemodynamic modes associated with interictal epileptic activity using a deformable model-based analysis of combined EEG and functional MRI recordings. *Hum Brain Mapp* 2010;31:1157–1173.
37. Storti SF, Formaggio E, Bertoldo A, et al. Modelling hemodynamic response function in epilepsy. *Clin Neurophysiol* 2013;124:2108–2118.
38. Friston KJ, Harrison L, Penny W. Dynamic causal modelling. *NeuroImage* 2003;19:1273–1302.
39. Murta T, Leal A, Garrido MI, et al. Dynamic Causal Modelling of epileptic seizure propagation pathways: a combined EEG-fMRI study. *NeuroImage* 2012;62:1634–1642.
40. Vaudano AE, Carmichael DW, Salek-Haddadi A, et al. Networks involved in seizure initiation. A reading epilepsy case studied with EEG-fMRI and MEG. *Neurology* 2012;79:249–253.
41. Vaudano AE, Avanzini P, Tassi L, et al. Causality within the epileptic network: an EEG-fMRI study validated by intracranial EEG. *Front Neurol* 2013;4:185.
42. Klamer S, Rona S, Elshahabi A, et al. Multimodal effective connectivity analysis reveals seizure focus and propagation in musicogenic epilepsy. *NeuroImage* 2015;113:70–77.

Supporting Information

Additional supporting information may be found online in the Supporting Information section at the end of the article.

Figure S1. Activation pattern of BOLD signal changes preceding and following GSWDs in all patients. Activations are depicted in yellow and deactivations in blue ($p < 0.05$, corrected at cluster level).

Figure S2. Mean BOLD time courses during GSWDs in the 3 investigated networks and the thalamus.

Figure S3. DCM analysis of all subjects.

Table S1. GLM analysis on single-subject level depicting activations (+) and deactivations (−) for each subject (N = 12) at 16, 12, 8, 4, and 0 s before and 4 s after GSWD onset.

Table S2. DCM *F* values (i.e., negative log-evidence) for each model at single subject and group level.